Soft Intertrack Interference Cancellation for Two-Dimensional Magnetic Recording

Elnaz Banan Sadeghian and John R. Barry

School of Electrical and Computer Engineering, Georgia Institute of Technology, Atlanta, GA 30332 USA

We propose a detection strategy for the two-dimensional magnetic recording channel with multiple read heads, in which intertrack interference (ITI) is mitigated by a combination of linear combining and soft interference cancellation. The proposed strategy reduces the detection problem to a series of traditional one-dimensional detection problems, so that the existing iterative detection strategies based on turbo equalization may be leveraged. The performance of the proposed detector is compared with a previously reported detector, in which the ITI is suppressed linearly via a multiple-input equalizer. Numerical results demonstrate that the proposed detector outperforms the linear detector regardless of whether or not media noise is dominant, and further that the proposed detector is able to recover data from more tracks than is otherwise possible.

Index Terms— **2-D intersymbol interference (ISI), two-dimensional magnetic recording (TDMR), multiple-input multiple-output (MIMO), soft decision feedback.**

I. Introduction

THE combination of shingle write recording and data detection based on multiple readback waveforms is known as two-dimensional magnetic recording (TDMR), a promising technology for next-generation high-density data storage [1]. A key challenge for TDMR is the development of signal processing strategies of manageable complexity that are able to effectively mitigate both intertrack interference (ITI) in the crosstrack dimension and intersymbol interference (ISI) in the downtrack dimension.

There are two distinct models for TDMR detection that have arisen in the prior art: 1) *the two-dimensional (2-D) ISI* model, in which the relevant signals are modeled as 2-D signals indexed by two interchangeable variables, and 2) the *multiple-input multiple-output (MIMO)* model, in which the relevant signals are modeled as scalar-valued or vector-valued functions of *one* variable, nominally time. The choice of which model to use depends on the number N of readback waveforms that are to be processed simultaneously: the 2-D model arises when N is large, whereas the MIMO model arises when N is small. We remark that N_p passes over a sector by an array of N_r readers will result in a total of $N = N_p N_r$ readback waveforms, so that N can be significantly larger than the number of physical readers.

1) The **2-D model** arises when the number N of readback waveforms being processed is large, since in this case the relevant signals are naturally represented as 2-D signals. In particular, the bits written on the disk are represented as a 2-D signal (or in the finite case by a matrix), with the two dimensions (downtrack and crosstrack) being roughly comparable in size and interchangeable, so that the matrix is roughly square. Similarly, the sampled readback waveforms can be represented as 2-D signals or matrices, as can the 2-D impulse response that captures both the ITI and ISI. In its simplest form, the 2-D ISI model involves a 2-D convolution of the data matrix with the impulse response matrix.

   Detector design for the 2-D channel is an active area of research. The maximum-likelihood (ML) detector for the 2-D ISI channel is prohibitively complex; there is no 2-D analog of the Viterbi detector that enables optimal performance with low complexity [2]. A variety of sub-optimal detectors with reduced complexity have been proposed, many of which can be viewed as 2-D extensions of 1-D detectors. The detector in [3], for example, uses four 1-D decision-feedback equalizers (DFEs) to scan the 2-D signal in four different directions. The detector in [4] achieves near-ML performance by iterating between Bahl, Cocke, Jelinek and Raviv (BCJR) equalizer [5] for the rows and DFE for the columns of the 2-D signal. The detector of [6] iterates between a binary and a non-binary BCJR detector, respectively, for the rows and the columns of a coded 2-D signal on a separable 2-D ISI channel; this detector falls only 1 dB short of an interference-free channel and thereby encourages equalizing a general 2-D impulse response to a nearby separable matrix. A generalized belief propagation detector is proposed in [7] that exploits the data-dependent media noise. Several other detectors have been proposed based on iterative decision feedback, in which extrinsic information is exchanged in a turbo fashion between modified BCJR detectors, including the row and column soft decision feedback algorithm [8], iterative soft decision zig–zag algorithm [9], and a multi-row/column detector coupled with a 2-D equalizer [10].

2) The **MIMO model** arises when the number N of readback waveforms being processed is small. In practice, N can be very small, perhaps as small as $N = 2$, especially in low-latency applications that

Manuscript received April 8, 2014; revised September 4, 2014 and October 22, 2014; accepted November 18, 2014. Date of publication December 9, 2014; date of current version June 15, 2015. Corresponding author: E. Banan Sadeghian (e-mail: ebsadeghian@ece.gatech.edu).

Color versions of one or more of the figures in this paper are available online at http://ieeexplore.ieee.org.

Digital Object Identifier 10.1109/TMAG.2014.2379220

cannot tolerate the delay required by multiple passes over a sector. In fact, the first step toward TDMR will involve a single pass by a single slider with only $N = 2$ readers [11]–[13]. The key distinction of the MIMO model is that the relevant signals are modeled as scalar-valued or vector-valued functions of one variable, nominally time, rather than as 2-D signals.

Detector design for MIMO channels has been studied for more than a decade [13]–[17]. A variation of the MIMO model arises from the multi-track scenario in which the tracks are written in small groups, with guard bands between neighboring groups; this limits the number of inputs and avoids the problem of unknown boundary conditions [14]–[17]. For example, the performance of an ideal ML detector for the multi-track scenario was analyzed in [14]. A variety of low-complexity multi-track detectors have been proposed. For example, a method in [15] divides an low density parity check (LDPC) codeword into three segments and records them on three adjacent tracks. The detector then iteratively detects between three inner detectors and an outer decoder to recover three input tracks from $N = 3$ readback waveforms. The detector in [16] improves the recovery of the 2-D-equalized center track, from $N = 3$ signals, by first estimating the sidetracks and providing their ITI information to the center track detector. A recently proposed detector [17] recovers four input tracks from $N = 2$ readback waveforms using the joint detection and decoding of two parallel detectors concatenated with two parallel LDPC decoders. Another recent detector employs MMSE linear equalization to a 1-D target to recover the middle track from $N = 3$ readback waveforms [13].

The 2-D and MIMO models are different enough that detector designs for one are not directly applicable to the other. A connection between the 2-D model and the MIMO model is easily made: Starting with a 2-D ISI model based on a large number—say N'—of readback waveforms, the MIMO model can be derived by discarding all but N of the output waveforms. In particular, when the 2-D ISI channel output is represented as a matrix with N' rows, the MIMO channel output can be constructed by extracting a subset of N adjacent rows. From this simple observation, we see that the MIMO model differs from the 2-D model in the following fundamental ways, beyond just the notational distinction of using 1-D or 2-D signals:

1) In the MIMO model, the downtrack and crosstrack dimensions are not interchangeable, and the channel output matrix will not be square; instead the downtrack dimension will dominate, with perhaps many thousands of columns but only N rows.
2) The MIMO model can be underdetermined, in the sense that there may be more input tracks that contribute significantly to the readback waveforms than can be reliably detected. These undetectable interfering tracks represent unknown boundary conditions, a feature not present in the 2-D ISI model.

In this paper, we adopt the MIMO model for low-latency applications for the case when there are no guard bands, so that the number of contributing tracks is larger than the number N of readback waveforms (i.e. the system is underdetermined), and we propose an iterative soft ITI cancellation detector with the following features:

1) The proposed detector leverages well-established 1-D detectors to efficiently account for ISI without simultaneously accounting for ITI.
2) The proposed detector admits an iterative implementation in which a given track that has already been detected can be revisited and detected anew with improved performance.
3) The proposed detector is compatible with iterative detectors, enabling the power of error-control coding to be harnessed for the tasks of ITI and ISI mitigation.
4) The proposed detector enables reliable recovery of bits from tracks near the edge of the array of read heads; we present one example in which five adjacent tracks are reliably recovered from an array of $N = 5$ readers.
5) The proposed detector outperforms a detector that linearly suppresses ITI by equalizing the N waveforms to a 1-D target.

II. Model

We adopt a separable and linear model for the channel [14], [16] with both first-order jitter noise and electronic noise, so that the readback waveform from the ith read head is given by

$$r_i(t) = \sum_n g_{i,n} \Bigg(\sum_k a_k^{(n)} h(t - kT) + \big(a_k^{(n)} - a_{k-1}^{(n)}\big) j_k^{(n)} q(t - kT) \Bigg) + n_i(t) \quad (1)$$

where $a_k^{(n)} \in \{\pm 1\}$ is the kth coded bit of track n, T is the bit period, $h(t)$ is the bit response (assumed to be the same for all tracks), $j_k^{(n)}$ is the kth jitter noise component for track n, $q(t)$ is the derivative of the corresponding transition response, $g_{i,n}$ is the crosstrack response gain from track n at read head i, and $n_i(t)$ is the additive electronic noise for the ith read head. We assume that the jitter components $\{j_k^{(n)}\}$ are independent identically distributed zero-mean Gaussian random variables with a variance σ_j^2 that does not depend on the track index n. We assume that the electronic noise $n_i(t)$ is white and Gaussian with a power-spectral density of $N_0/2$, the same for all read heads.

Applying the ith readback waveform to an antialiasing filter and then sampling at the bit rate leads to

$$r_k^{(i)} = \sum_n g_{i,n} \big(x_k^{(n)} + m_k^{(n)}\big) + n_k^{(i)} \quad (2)$$

where $x_k^{(n)} = \sum_i a_i^{(n)} h_{k-i}$ is the "ISI symbol" sequence for track n, h_k is the kth sample of the filtered bit response, $m_k^{(n)} = \sum_i (a_i^{(n)} - a_{i-1}^{(n)}) j_i^{(n)} q_{k-i}$ is the data-dependent "media-noise" sequence for track n, q_k is the kth sample of the filtered derivative of the transition response, and $n_k^{(i)}$ is the kth sample of the filtered electronic noise $n_i(t)$, with zero mean and variance $N_0/(2T)$.

Collecting the N samples from each of the N read heads at time k into the vector $\mathbf{r}_k = [r_k^{(1)}, \ldots, r_k^{(N)}]^T$, and using (2), we arrive at a MIMO model for the TDMR channel

$$\mathbf{r}_k = \sum_n \left(x_k^{(n)} + m_k^{(n)}\right)\mathbf{g}_n + \mathbf{n}_k \tag{3}$$

where $\mathbf{n}_k = [n_k^{(1)}, n_k^{(2)}, \ldots, n_k^{(N)}]^T$ and $\mathbf{g}_n = [g_{1,n}, g_{2,n}, \ldots, g_{N,n}]^T$. In this MIMO model, the number of outputs is N, the number of read heads, and the number of inputs is the number of relevant tracks that contribute to the output vector $\mathbf{r}_k$, a number that depends on the extent of the crosstrack response $\{g_{i,n}\}$. For example, if $\{g_{i,n}\} = 0$ for $n > L$, then the number of inputs (contributing tracks) is L.

The per-bit SNR for the ith track, ignoring the ITI from other tracks, can be computed from (3) as

$$\mathrm{SNR}_i = \frac{E_h}{N_0/\|\mathbf{g}_i\|^2 + M_0} \tag{4}$$

where $E_h = E_x T$ is the energy of the bit response $h(t)$, expressed in terms of the variance $E_x = E((x_k^{(n)})^2)$ of the ISI symbols, and $M_0 = 4T\sigma_j^2 E_q$ is the equivalent single-sided rectangular power spectrum of the media noise [18], expressed in terms of $E_q = \sum_k q_k^2$. Each track will have a different $\mathbf{g}_i$ and thus a different SNR; depending on the array geometry and noise statistics, tracks closer to the center of the read-head array will likely have a higher SNR than those near the edge.

III. Two Detection Strategies

We describe two strategies for mitigating ITI: 1) linear suppression and 2) a combination of linear suppression, and soft interference cancellation.

A. Linear ITI Suppression

ITI can be suppressed linearly by taking a memoryless linear combination of the N read-head samples at each time k, as illustrated in Fig. 1 [13], [16]. The combining weights will depend on which track is being detected. In particular, if the goal is to detect track i, then we form the following linear combination:

$$y_k^{(i)} = \mathbf{w}_i^T \mathbf{r}_k \tag{5}$$

where $\mathbf{w}_i$ is a vector of combining weights for track i. Since the aim of these weights is to suppress ITI alone (and not ISI and media noise, for example), a reasonable optimization criterion is to choose the weights to minimize the mean-squared error between the resulting linear combination and the desired noiseless ISI symbol plus media noise sample, namely

$$\mathrm{MSE} = E\left(\left(y_k^{(i)} - \left(x_k^{(i)} + m_k^{(i)}\right)\right)^2\right). \tag{6}$$

As shown in Appendix A, the weights that minimize this MSE are

$$\mathbf{w}_i = \left(\sum_n \mathbf{g}_n \mathbf{g}_n^T + \left(\frac{N_0}{2E_h + M_0}\right)\mathbf{I}\right)^{-1} \mathbf{g}_i. \tag{7}$$

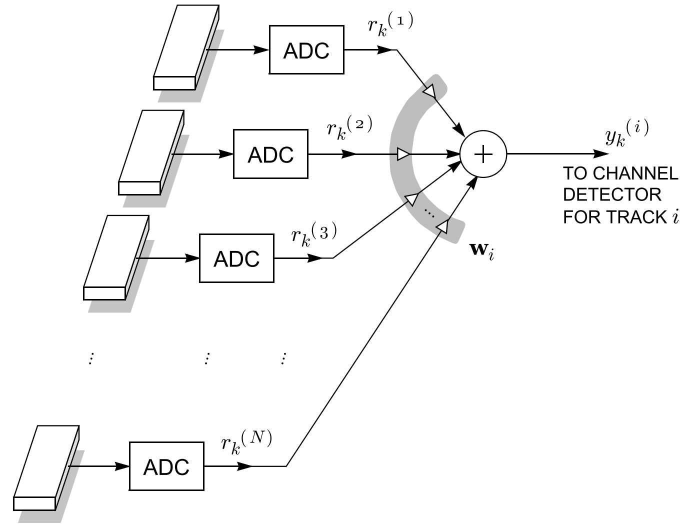

Fig. 1. Linear suppression of ITI using an array of N read heads.

When there is more than one track to be detected, the same linear ITI suppression strategy may be applied separately for each individual track.

If we substitute (3) into (5), we find that

$$y_k^{(i)} = x_k^{(i)}\mathbf{w}_i^T\mathbf{g}_i + \sum_{n\neq i} x_k^{(n)}\mathbf{w}_i^T\mathbf{g}_n + \sum_n m_k^{(n)}\mathbf{w}_i^T\mathbf{g}_n + \mathbf{w}_i^T\mathbf{n}_k. \tag{8}$$

The first term includes an undesirable factor $\mathbf{w}_i^T\mathbf{g}_i$ that can be interpreted as a *bias*; removing the bias yields

$$y_k^{(i)}/\left(\mathbf{w}_i^T\mathbf{g}_i\right) = x_k^{(i)} + \eta_k^{(i)} \tag{9}$$

where $\eta_k^{(i)} = (\sum_{n\neq i} x_k^{(n)}\mathbf{w}_i^T\mathbf{g}_n + \sum_n m_k^{(n)}\mathbf{w}_i^T\mathbf{g}_n + \mathbf{w}_i^T\mathbf{n}_k)/(\mathbf{w}_i^T\mathbf{g}_i)$ is the sum of the residual interference, jitter noise, and electronic noise, whose variance is

$$\sigma_\eta^{2(i)} = \frac{1}{2T} \times \frac{\left(2E_h\sum_{n\neq i}\left(\mathbf{w}_i^T\mathbf{g}_n\right)^2 + M_0\sum_n\left(\mathbf{w}_i^T\mathbf{g}_n\right)^2 + N_0\|\mathbf{w}_i\|^2\right)}{\left(\mathbf{w}_i^T\mathbf{g}_i\right)^2}. \tag{10}$$

The model in (9) looks like a conventional 1-D recording model, with an ISI sequence from track i corrupted by media and additive noise, and it can be detected using any of a variety of standard techniques, including the Viterbi detector, the BCJR detector, a pattern-dependent noise-predictive detector [18], or an iterative detector, such as a turbo equalizer that iterates between a channel detector and an error-control decoder [19] (Section IV).

B. Soft ITI Cancellation

Successive interference cancellation using hard decisions is an effective multi-user detection strategy that was originally conceived for CDMA applications [20], [21]. Successive cancellation using soft decisions can lead to improved performance [22]–[25]. We apply the concept of successive interference cancellation using soft decisions to TDMR. In particular, as described below, we propose to detect tracks one at a time, and cancel ITI from previously detected tracks using soft decisions, while accounting for the reliability of previous decisions.

An important degree of freedom for the proposed detector is the *detection order*, since the order in which tracks are detected will significantly impact performance. We will represent the detection order by an ordered list $\mathbf{\Pi}$ of track indices, where the first entry of the list is the index of the track detected first, the second entry is the index of the track detected second, and so on.

There may be an advantage in detecting a particular track more than once, and thus we allow for repeated entries in $\mathbf{\Pi}$. For example, $\mathbf{\Pi} = [1, 2, 3, 2, 1]$ would mean that we first detect track 1, then track 2, then track 3, then we redetect track 2, and finally we redetect track 1. We note that a repeated detection for a given track is an option, not a necessity, and further that when it does occur it is based on the original set of readback waveforms, not a new set based on a rescan of the disk. In other words, the entire algorithm operates on a single set of sampled waveforms from a single pass of the readers over the track(s) of interest. Although performance can be improved when a second set of waveforms is made available through a repeated pass of the readers, at the cost of increased delay, this paper does not consider such extensions.

Suppose we are currently interested in detecting track i. Let $\mathcal{P}$ denote the index set of the previously detected tracks, excluding the current track i. To detect track i, we will *softly* cancel the interference caused by the set $\mathcal{P}$ while linearly suppressing any ITI that remains. In particular, we propose to first subtract a soft estimate of the interference from the previously detected tracks in $\mathcal{P}$ before taking a linear combination, according to

$$y_k^{(i)} = \mathbf{w}_i^T \left(\mathbf{r}_k - \sum_{n \in \mathcal{P}} \tilde{x}_k^{(n)} \mathbf{g}_n \right). \tag{11}$$

This equation captures the essence of the proposed soft ITI cancellation scheme. Here, $\tilde{x}_k^{(n)}$ denotes a soft estimate of the kth ISI symbol $x_k^{(n)}$ from the previously detected track n, which is computed by convolving a sequence of soft estimates $\{\tilde{a}_k^{(n)}\}$ for the bits with the ISI response, according to the following lemma.

Lemma 1: Let $\lambda_k^{(n)} = \ln(P(a_k^{(n)} = 1|\{\mathbf{r}_i\})/P(a_k^{(n)} = -1|\{\mathbf{r}_i\}))$ denote the kth *a posteriori* log-likelihood ratio (LLR) for track n. Given knowledge of $\{\lambda_k^{(n)}$: for all $k\}$, the soft estimate $\tilde{x}_k^{(n)}$ that minimizes the mean-squared error $E((\tilde{x}_k^{(n)} - x_k^{(n)})^2|\{\lambda_k^{(n)}\})$ is

$$\tilde{x}_k^{(n)} = \sum_i \tilde{a}_i^{(n)} h_{k-i} \tag{12}$$

where $\tilde{a}_k^{(n)} = \tanh(\lambda_k^{(n)}/2)$.

Proof: Setting to zero the partial derivative of $E((\tilde{x}_k^{(n)} - x_k^{(n)})^2|\{\lambda_k^{(n)}\})$ with respect to $\tilde{x}_k^{(n)}$ leads to the result that the estimate that minimizes the mean-squared error is the conditional mean

$$\begin{aligned} \tilde{x}_k^{(n)} &= E\big(x_k^{(n)}|\{\lambda_k^{(n)}\}\big) && (13)\\ &= E\left(\sum_i a_i^{(n)} h_{k-i}|\{\lambda_k^{(n)}\}\right) && (14)\\ &= \sum_i E\big(a_i^{(n)}|\{\lambda_k^{(n)}\}\big) h_{k-i} && (15)\\ &= \sum_i \tilde{a}_i^{(n)} h_{k-i} && (16)\end{aligned}$$

where we have introduced the conditional mean $\tilde{a}_k^{(n)} = E(a_k^{(n)}|\{\lambda_k^{(n)}\})$, which is well-known to reduce to $\tilde{a}_k^{(n)} = \tanh(\lambda_k^{(n)}/2)$ [26]. ■

Here, two extreme cases are noteworthy. In the extreme case when a previously detected track n has an infinite SNR, the resulting soft estimates $\tilde{x}_k^{(n)}$ will exactly match the actual $x_k^{(n)}$. In this case, the soft cancellation in (11) reduces to hard cancellation, and it will completely remove the influence of the ISI symbols of track n. At the other extreme, if track n has a zero SNR, the resulting LLR and soft decisions will also be zero. In this case, the soft cancellation in (11) will subtract zero, which means it will not do any cancellation at all. In practice, of course, the SNR will be between the two extremes, so that in practice the cancellation will be only partial—residual ITI will remain even after the soft cancellation process.

In (11), we see that, after the soft cancellation of ITI from previously detected tracks, the combining weights $\mathbf{w}_i$ are used to linearly suppress any ITI that remains. This includes not only ITI from as-yet undetected tracks, but also residual ITI that remains after the soft cancellation process from previously detected tracks.

In Appendix B, we show that the linear combining weights that minimize the MSE after soft cancellation of the previously detected tracks are

$$\mathbf{w}_i = \left(\sum_n \left(\frac{\alpha_n 2E_h + M_0}{2E_h + M_0} \right) \mathbf{g}_n \mathbf{g}_n^T + \left(\frac{N_0}{2E_h + M_0} \right) \mathbf{I} \right)^{-1} \mathbf{g}_i \tag{17}$$

where

$$\alpha_n = \begin{cases} 1, & \text{for } n \notin \mathcal{P} \\ E\big((x_k^{(n)} - \tilde{x}_k^{(n)})^2\big)/E_x, & \text{for } n \in \mathcal{P}. \end{cases} \tag{18}$$

For $n \in \mathcal{P}$, we can interpret α_n as a reliability factor, since it is a number between 0 and 1 that quantifies the reliability of the decisions from track n. Two extreme cases lend insight as follows:

1) At one extreme, $\alpha_n = 1$ corresponds to the case where the decisions of track n are completely unreliable; in this case, the weight computation in (17) will treat track n as an undetected track. Observe that for the special case when $\alpha_n = 1$ for all tracks (which happens when no tracks have been previously detected, so that $\mathcal{P}$ is the empty set), the weights in (17) reduce to the linear weights of (7).
2) At the other extreme, $\alpha_n = 0$ corresponds to the case where track n produces completely reliable decisions,

in which case the cancellation in (11) of the ISI symbols from track n is perfect; nevertheless, there will always be media noise from track n that is not canceled by (11), and for this reason, the contribution from track n to the weights in (17) is small when $\alpha_n = 0$, but not zero.

Note that when detecting the very first track, there will be no previously detected tracks, so that $\mathcal{P}$ is empty. In this case, (11) reduces to the linear detector, and the weights of (17) reduce to the linear weights from (7). Thus, it follows that, in the proposed soft ITI cancellation scheme, the first track is detected linearly.

As in the linear case, we must account for the bias of the MMSE weights. Substituting (3) into (11) yields

$$y_k^{(i)} = \mathbf{w}_i^T \mathbf{g}_i x_k^{(i)} + \mathbf{w}_i^T \times \left(\sum_{n \neq i} x_k^{(n)} \mathbf{g}_n + \sum_n m_k^{(n)} \mathbf{g}_n + \mathbf{n}_k - \sum_{n \in \mathcal{P}} \tilde{x}_k^{(n)} \mathbf{g}_n \right). \tag{19}$$

To remove the bias evident in the first term, we divide through by the constant $\mathbf{w}_i^T \mathbf{g}_i$, yielding

$$z_k^{(i)} = x_k^{(i)} + \eta_k^{(i)} \tag{20}$$

where $z_k^{(i)} = y_k^{(i)} / (\mathbf{w}_i^T \mathbf{g}_i)$, and where

$$\eta_k^{(i)} = \mathbf{w}_i^T \left(\sum_{n \neq i, n \notin \mathcal{P}} x_k^{(n)} \mathbf{g}_n + \sum_{n \in \mathcal{P}} \left(x_k^{(n)} - \tilde{x}_k^{(n)} \right) \mathbf{g}_n + \sum_n m_k^{(n)} \mathbf{g}_n + \mathbf{n}_k \right) \Big/ \left(\mathbf{w}_i^T \mathbf{g}_i \right). \tag{21}$$

Here, η_k is the sum of noise and residual interference. In particular, the first term in (21) is the ITI from tracks that have not yet been detected, the second term is the residual ITI that is left after soft cancellation from previously detected tracks, the third term is the media noise from all tracks, and the last term is the electronic noise. The variance of the noise-plus-interference is

$$\sigma_\eta^{2(i)} = \frac{1}{2T} \left(2E_h \sum_{n \neq i} \alpha_n \left(\mathbf{w}_i^T \mathbf{g}_n \right)^2 + M_0 \sum_n \left(\mathbf{w}_i^T \mathbf{g}_n \right)^2 + N_0 \|\mathbf{w}_i\|^2 E_h \right) \Big/ \left(\mathbf{w}_i^T \mathbf{g}_i \right)^2. \tag{22}$$

The pseudocode of the proposed algorithm is shown in Algorithm 1. The inputs to the algorithm are the analog to digital converter (ADC) outputs, the ITI response, the ISI response, and the detection order $\mathbf{\Pi}$. The output of the algorithm is the set of *a posteriori* LLRs for each track in $\mathbf{\Pi}$.

The algorithm begins by initializing $\alpha_n = 1$ for all tracks n. It then proceeds to the main loop (line 2 through line 11), which steps through each track index in $\mathbf{\Pi}$. The current track index is identified as i in line 3, and the set of previously detected tracks that will be used for cancellation is identified as $\mathcal{P}$ in line 4. Observe that line 4 specifically excludes the current track i from $\mathcal{P}$, which is necessary if track i were detected earlier, since it would not make sense to subtract the contributions from track i when the goal is to detect track i.

Algorithm 1: Pseudocode of the Proposed Soft ITI Cancellation Detector

Inputs: ADC outputs $\{\mathbf{r}_k\}$
Crosstrack and downtrack responses $\{\mathbf{g}_n\}$, $\{h_k\}$
Detection order $\mathbf{\Pi}$
Output: LLR's $\{\lambda_k^{(i)}\}$ for all detected tracks $i \in \mathbf{\Pi}$
1 **Init**: $\alpha_n = 1$ for all n
2 **for** $j = 1$ **to** $|\mathbf{\Pi}|$ **do**
3 $\quad i = \Pi(j)$
4 $\quad \mathcal{P} = \{\Pi(1), \ldots, \Pi(j-1)\} \backslash \{i\}$
5 $\quad \mathbf{w}_i = \left(\mathbf{g}_i \mathbf{g}_i^T + \sum_{n \neq i} (\alpha_n 2E_h + M_0)\, \mathbf{g}_n \mathbf{g}_n^T + N_0 \mathbf{I} \right)^{-1} (2E_h + M_0)\, \mathbf{g}_i$
6 $\quad z_k^{(i)} = \mathbf{w}_i^T \left(\mathbf{r}_k - \sum_{n \in \mathcal{P}} \tilde{x}_k^{(n)} \mathbf{g}_n \right) / \left(\mathbf{w}_i^T \mathbf{g}_i \right)$ for all k
7 $\quad$ Compute σ_η^2 using (22)
8 $\quad \{\lambda_k^{(i)}\} =$ Detect $(\{z_k^{(i)}\}, \{h_k\}, \sigma_\eta^2)$
9 $\quad \{\tilde{x}_k^{(i)}\} =$ Convolve $(\{\tanh(\lambda_k^{(i)}/2)\}, \{h_k\})$
10 $\quad \alpha_i = E((x_k^{(i)} - \tilde{x}_k^{(i)})^2)/E_x$
11 **end**

Observe further from line 4 that the first time through the main loop ($j = 1$), $\mathcal{P}$ will be the empty set.

The weights are computed using (17) in line 5, and the ITI cancellation and suppression is performed using (11) and $z_k^{(i)} = y_k^{(i)} / (\mathbf{w}_i^T \mathbf{g}_i)$ in line 6. After canceling and suppressing the ITI, the result is applied to a 1-D detector in line 8; this might be Viterbi, BCJR, or an iterative detector that iterates between a channel detector and the error-control decoder. Soft estimates of the ISI symbols are computed in line 9, which will be used in later passes through the main loop to cancel ITI. The reliability measure for these decisions is computed in line 10.

As written, the algorithm requires explicit knowledge of the target downtrack response $\mathbf{h}$, the crosstrack responses $\{\mathbf{g}_n\}$, the reliability parameters $\{\alpha_n\}$, the jitter variance σ_j^2, and the electronic noise power N_0. So as to quantify the ultimate performance of the proposed architecture, we assume in the following section that all of these parameters are known. While an adaptive implementation is beyond the scope of this paper, we should mention that straightforward adaptive estimation algorithms will be needed in practice for some of these parameters. For example, the crosstrack response $g_{i,j}$ from track j to reader i can be estimated by exploiting the knowledge of the preamble and other known patterns on track j, and using any of a variety of estimation strategies operating on the readback waveform from reader i, including recursive-least-square and least-mean-square algorithms [27] and per-survivor algorithms [28]. The downtrack response is typically the outcome of a joint optimization of target and equalizer based on the generalized partial response strategy [29]. The reliability parameter α_n can be estimated in at least two ways: First, it could be directly adapted to minimize the mean-squared error after soft cancellation using, for example, the least-mean-square algorithm. Alternatively, since α_n is a well-behaved function of the SNR for track n, it

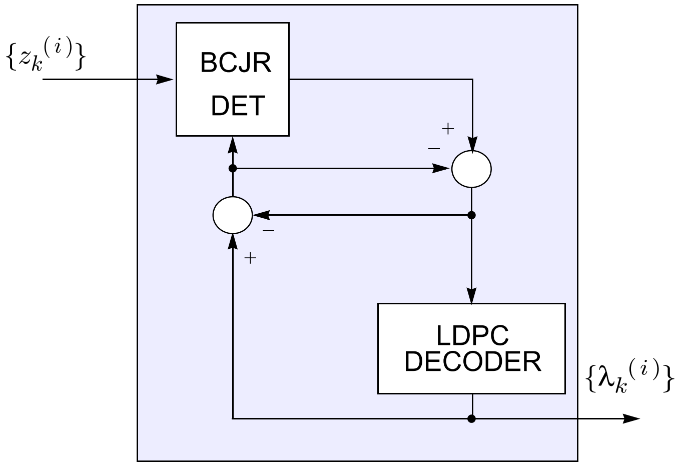

Fig. 2. Iterative detector based on turbo equalization [19].

may be simpler to first use training to establish a lookup table that maps SNR_n to α_n, and then during the detection process, use an estimate of SNR_n to lookup the corresponding α_n.

IV. Numerical Results

In this section, we present numerical results for evaluating the performance of the proposed detector. The results are based on the model (3) in the special case where there are $N = 5$ read heads and $L = 9$ inputs. We assume that the tracks are coded independently by a rate-0.9 regular LDPC code of length 36 409 and column weight 3, constructed using the progressive edge growth method [30]. Thus, the per-bit SNR for track i from (4) after accounting for the rate-R code becomes

$$\text{SNR}_i = \frac{E_h/R}{N_0/\|\mathbf{g}_i\|^2 + M_0}. \tag{23}$$

In the downtrack direction, we assume the E2PR2 ISI response $\mathbf{h} = [h_0, \ldots, h_4] = [1, 4, 6, 4, 1]$. We further assume that the five read heads are centered over five adjacent tracks, and that each reader exhibits the same Gaussian crosstrack response, namely, $\mathbf{g}_5^T = [g_{1,5}, \ldots, g_{5,5}] = [0.0183, 0.3679, 1, 0.3679, 0.0183]$ and $\mathbf{g}_{5-i}^T = [g_{1+i,5}, \ldots, g_{5+i,5}]$ for $|i| \le 4$.

In our numerical results, the 1-D detector of line 8 is implemented using the iterative detector shown in Fig. 2, in which a BCJR soft-output channel detector iterates with a soft-output LDPC decoder according to the turbo equalization principle [19]. Note that the BCJR detector does not exploit the data-dependence of the media noise; we expect improved performance using a pattern-dependent noise-predictive BCJR [18]. We implement 10 inner iterations (inside the LDPC decoder) for each outer iteration of the turbo equalizer. We apply the termination criterion from [31]: the iterative process continues as long as $\sum_k |\lambda_k^{(i)}|$ increases, and it stops as soon as it decreases.

We consider first the performance in the absence of media noise ($\sigma_j^2 = 0$), so that the relative media noise power $\gamma = M_0/(N_0 + M_0)$ reduces to $\gamma = 0$. The resulting frame error rate (FER) performance is shown in Fig. 3 for three different detectors: 1) the linear detector; 2) a hard ITI cancellation detector; and 3) the soft ITI cancellation detector.

First, we focus on the case when all tracks are detected using linear ITI suppression, which are the dashed gray curves in the figure. The two outer tracks[1] (i.e., tracks ± 2) never stray from an FER near unity over the range of SNR values shown; to achieve FER $< 10^{-2}$ for the outer tracks requires $\text{SNR}_0 = 40$ dB (not shown). The middle track (track 0) achieves FER $= 10^{-3}$ at $\text{SNR}_0 = 13.6$ dB, while the other two inner tracks (tracks ± 1) require 15.4 dB, a 1.8 dB difference.

Fig. 3 also includes the results of the proposed soft cancellation detector, which are the solid black curves in the figure. These results are based on a detection order of $\mathbf{\Pi} = [0, 1, -1, 0, 1, 2, 1, 0, -1, -2, -1, 0]$, so that the middle track is detected first and last, with all remaining tracks detected at least once along the way (among other candidate detection orders we considered, this performed the best. The problem of optimizing $\mathbf{\Pi}$ to maximize performance is an open problem). The performance for the middle track is only 0.2 dB better with soft ITI cancellation than with linear suppression: the middle track (track 0) with soft ITI cancellation achieves FER $= 10^{-3}$ at $\text{SNR}_0 = 13.4$ dB. However, soft ITI cancellation improves performance for the remaining tracks. In particular, the two inner tracks (tracks ± 1) perform identically to the middle track (track 0) with soft ITI cancellation. Thus, for the two inner tracks, the soft ITI cancellation detector outperforms the linear detector by 2 dB. The improvement from soft cancellation is even more dramatic for the outer tracks: with soft ITI cancellation, the outer tracks (tracks ± 2) achieve FER $= 10^{-3}$ at $\text{SNR}_0 = 17.6$ dB, which is only 4.2 dB worse than the center track, and over 22 dB better than can be achieved with linear detection alone. These results suggest that, at least in this one example, the advantage of the soft ITI cancellation strategy is not so much its performance for the inner tracks, but rather its advantage is its ability to reliably recover data from more tracks than is otherwise possible.

The solid gray curves in Fig. 3 show the performance of a *hard* ITI cancellation detector, which mimics the proposed soft ITI cancellation detector except with hard decisions $\tilde{a}_k^{(n)} = \text{sign}(\lambda_k^{(n)})$ used in place of soft decisions $\tilde{a}_k^{(n)} = \tanh(\lambda_k^{(n)}/2)$. The hard cancellation detector performs about 0.2 dB worse than the soft cancellation detector for the three inner tracks. Although the benefit of using soft decisions for ITI cancellation is modest in this example, the fact that the benefit comes at essentially no cost in complexity makes it attractive nonetheless.

Next, we consider the performance when the media noise accounts for 80% of the total noise power, so that $\gamma = M_0/(N_0 + M_0) = 0.8$. All other parameters remain the same as before. The resulting performance is shown in Fig. 4.

Consider first the linear detector: Similar to the case with $\gamma = 0$, we observe that the two outer tracks are not recovered reliably for the range of SNR values shown. We also observe that the middle track (track 0) and the other two inner tracks (tracks ± 1) achieve FER $= 10^{-3}$ at

[1]For convenience we renumber the tracks: track 0 is the center track, tracks ± 1 are its neighbors, etc.

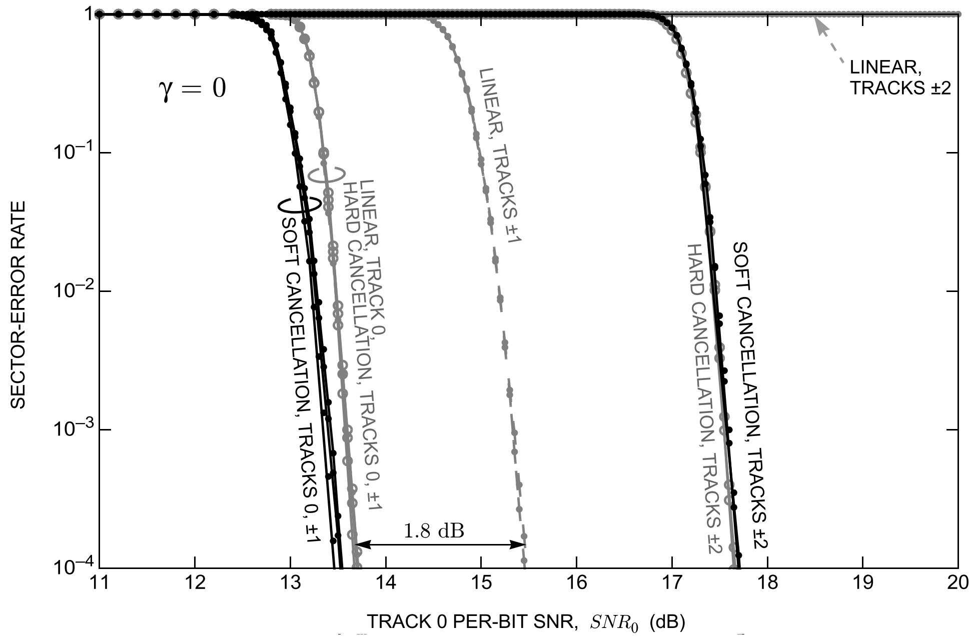

Fig. 3. FER performance in the absence of media noise ($\gamma = 0$).

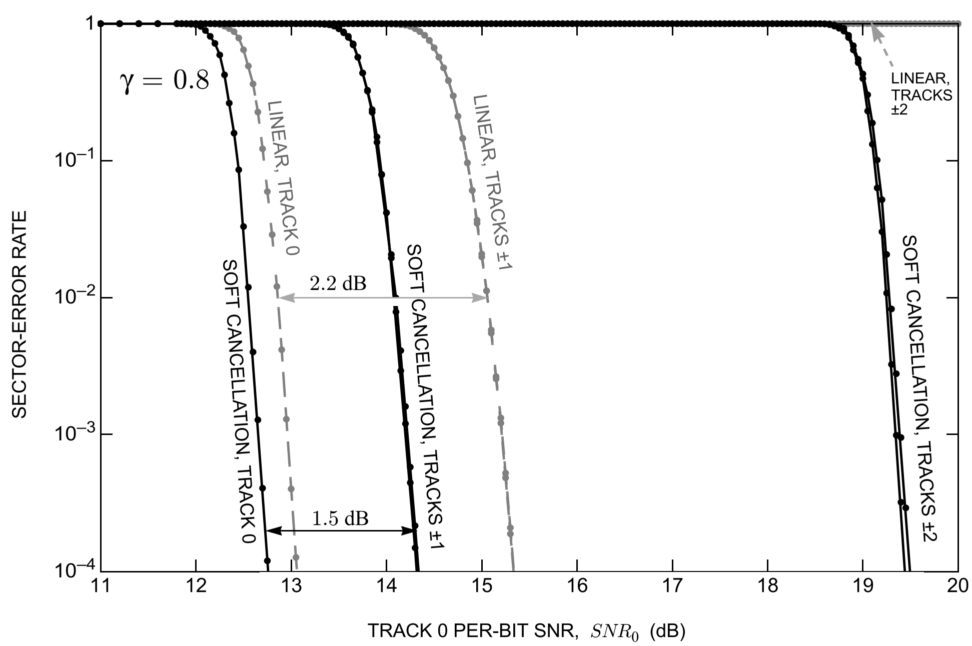

Fig. 4. FER performance when media noise is dominant ($\gamma = 0.8$).

$\text{SNR}_0 = 13$ dB and 15.2 dB, respectively. With soft ITI cancellation, however, we can recover the two outer tracks with $\text{FER} = 10^{-3}$ at $\text{SNR}_0 = 19.4$ dB, the two inner tracks at $\text{SNR}_0 = 14.2$ dB, and the middle track at $\text{SNR}_0 = 12.7$ dB. The performance gain for the soft cancellation detector thus depends on the track: it is a modest 0.3 dB for track 0, but it grows to 1.0 dB for tracks ± 1.

A comparison of Figs. 3 and 4 reveals insight into how the two detection strategies react to media noise. In particular, as the media noise ratio increases from $\gamma = 0$ to $\gamma = 0.8$, we observe the following:

1) For the linear detector, the penalty for tracks ± 1 (relative to track 0) jump from 1.8 to 2.2 dB.
2) For the soft ITI canceller, the penalty for tracks ± 1 (relative to track 0) jump from 0 to 1.5 dB.
3) For the soft ITI canceller, the penalty for tracks ± 2 (relative to track 0) jump from 4.2 to 6.7 dB.

The increased penalties in the face of media noise can be explained in part by the absence of any mechanism in the proposed algorithm for estimating and canceling the interference caused by media noise from interfering tracks.

V. Conclusion

We considered the problem of how to process the readback waveforms coming from an array of two or more read heads in a TDMR application. We presented two strategies for mitigating the ITI, one based on linear suppression and one based on soft cancellation. Numerical results demonstrated that the relative advantage of the two detection strategies depends on the location of the track being detected. For the inner tracks near the center of the read-head array, the gain of the soft ITI cancellation detector over the linear detector is modest. For the outer tracks near the edge of the array, in contrast, the gain of the soft ITI cancellation detector over the linear detector is significant. Therefore, for a given pass of a read-head array, the soft ITI cancellation strategy has demonstrated its ability to reliably recover the data from more tracks than would otherwise be possible using linear ITI suppression. Future work should develop adaptive implementations for these algorithms and explore the optimization problem for the detection order $\boldsymbol{\Pi}$.

Appendix A
Derivation of (7) for Linear Case

For the case of linear ITI suppression of (5), the mean-squared error of (6) can be written as

$$\begin{aligned}\text{MSE} &= E\big(\big(\mathbf{w}_i^T\mathbf{r}_k - \big(x_k^{(i)} + m_k^{(i)}\big)\big)^2\big)\\ &= \mathbf{w}_i^T E\big(\mathbf{r}_k\mathbf{r}_k^T\big)\mathbf{w}_i + E_x + 2\sigma_j^2 E_q\\ &\quad -2\mathbf{w}_i^T E\big(\big(x_k^{(i)} + m_k^{(i)}\big)\mathbf{r}_k\big)\\ &= \mathbf{w}_i^T\mathbf{R}\mathbf{w}_i + E_x + 2\sigma_j^2 E_q - 2\mathbf{w}_i^T\mathbf{p} &(24)\\ &= (\mathbf{w}_i - \mathbf{R}^{-1}\mathbf{p})^T\mathbf{R}(\mathbf{w}_i - \mathbf{R}^{-1}\mathbf{p}) + E_x\\ &\quad + 2\sigma_j^2 E_q - \mathbf{p}^T\mathbf{R}^{-1}\mathbf{p} &(25)\end{aligned}$$

where we have introduced the correlation matrix $\mathbf{R} = E(\mathbf{r}_k\mathbf{r}_k^T)$ and correlation vector $\mathbf{p} = E((x_k^{(i)} + m_k^{(i)})\mathbf{r}_k)$, and where the last equality follows from completing the square. From (3), we can compute $\mathbf{R}$ and $\mathbf{p}$ as

$$\begin{aligned}\mathbf{R} &= \big(E_x + 2\sigma_j^2 E_q\big)\sum_n \mathbf{g}_n\mathbf{g}_n^T + \left(\frac{N_0}{2T}\right)\mathbf{I}, \text{ and}\\ \mathbf{p} &= \big(E_x + 2\sigma_j^2 E_q\big)\mathbf{g}_i. &(26)\end{aligned}$$

Since $\mathbf{R}$ is symmetric, the quadratic form for the first term in (25) implies that it cannot be negative. We can thus minimize MSE by forcing the first term to zero, which is achieved when $\mathbf{w}_i = \mathbf{R}^{-1}\mathbf{p}$, which reduces to (7) when using the results of (26), along with the identity $M_0 = 4T\sigma_j^2 E_q$.

Appendix B
Derivation of (17)

The defining equation of (11) for the soft ITI cancellation scheme can be rewritten as

$$y_k^{(i)} = \mathbf{w}_i^T\tilde{\mathbf{r}}_k \tag{27}$$

where we have introduced $\tilde{\mathbf{r}}_k$ the residual observation vector after soft cancellation, namely

$$\tilde{\mathbf{r}}_k = \mathbf{r}_k - \sum_{n\in\mathcal{P}} \tilde{x}_n^{(n)}\mathbf{g}_n. \tag{28}$$

Therefore, following the same procedure as in Appendix A, we can write the MSE after soft ITI cancellation as

$$\begin{aligned}\text{MSE} &= (\mathbf{w}_i - \tilde{\mathbf{R}}^{-1}\mathbf{p})^T\tilde{\mathbf{R}}(\mathbf{w}_i - \tilde{\mathbf{R}}^{-1}\mathbf{p})\\ &\quad + E_x + 2\sigma_j^2 E_q - \mathbf{p}^T\tilde{\mathbf{R}}^{-1}\mathbf{p} &(29)\end{aligned}$$

where from (3) and (28) we have

$$\begin{aligned}\mathbf{p} &= E\big(\big(x_k^{(i)} + m_k^{(i)}\big)\tilde{\mathbf{r}}_k\big)\\ &= E\big(\big(x_k^{(i)} + m_k^{(i)}\big)\mathbf{r}_k\big)\\ &= \big(E_x + 2\sigma_j^2 E_q\big)\mathbf{g}_i &(30)\end{aligned}$$

and

$$\begin{aligned}\tilde{\mathbf{R}} &= E\big(\tilde{\mathbf{r}}_k\tilde{\mathbf{r}}_k^T\big)\\ &= E_x\sum_{n\notin\mathcal{P}}\mathbf{g}_n\mathbf{g}_n^T + \sum_{n\in\mathcal{P}} E\Big(\big(x_k^{(n)} - \tilde{x}_k^{(n)}\big)^2\Big)\mathbf{g}_n\mathbf{g}_n^T\\ &\quad +2\sigma_j^2 E_q\sum_n \mathbf{g}_n\mathbf{g}_n^T + \left(\frac{N_0}{2T}\right)\mathbf{I}\\ &= E_x\sum_n \alpha_n\mathbf{g}_n\mathbf{g}_n^T + 2\sigma_j^2 E_q\sum_n \mathbf{g}_n\mathbf{g}_n^T + \left(\frac{N_0}{2T}\right)\mathbf{I} &(31)\end{aligned}$$

where we have introduced

$$\alpha_n = \begin{cases}1, & \text{for } n\notin\mathcal{P}\\ E\Big(\big(x_k^{(n)} - \tilde{x}_k^{(n)}\big)^2\Big)/E_x, & \text{for } n\in\mathcal{P}.\end{cases} \tag{32}$$

We can thus minimize MSE by forcing the first term in (29) to zero, which is achieved when $\mathbf{w}_i = \tilde{\mathbf{R}}^{-1}\mathbf{p}$. This reduces to (17) when using (30) and (31).

References

[1] R. Wood, M. Williams, A. Kavcic, and J. Miles, "The feasibility of magnetic recording at 10 terabits per square inch on conventional media," *IEEE Trans. Magn.*, vol. 45, no. 2, pp. 917–923, Feb. 2009.

[2] E. Ordentlich and R. M. Roth, "On the computational complexity of 2D maximum-likelihood sequence detection," Hewlett-Packard Labs, Palo Alto, CA, USA, Tech. Rep. HPL-2006-69, 2006.

[3] J. K. Nelson, A. C. Singer, and U. Madhow, "Multi-directional decision feedback for 2D equalization," in *Proc. IEEE Int. Conf. Acoust., Speech, Signal Process.*, vol. 4. May 2004, pp. IV-921–IV-924.

[4] M. Marrow and J. K. Wolf, "Iterative detection of 2-dimensional ISI channels," in *Proc. IEEE Inf. Theory Workshop*, Paris, France, Mar./Apr. 2003, pp. 131–134.

[5] L. Bahl, J. Cocke, F. Jelinek, and J. Raviv, "Optimal decoding of linear codes for minimizing symbol error rate (Corresp.)," *IEEE Trans. Inf. Theory*, vol. 20, no. 2, pp. 284–287, Mar. 1974.

[6] Y. Wu, J. A. O'Sullivan, R. S. Indeck, and N. Singla, "Iterative detection and decoding for separable two-dimensional intersymbol interference," *IEEE Trans. Magn.*, vol. 39, no. 4, pp. 2115–2210, Jul. 2003.

[7] S. M. Khatami and B. Vasic, "Generalized belief propagation detector for TDMR microcell model," *IEEE Trans. Magn.*, vol. 49, no. 7, pp. 3699–3702, Jul. 2013.

[8] T. Cheng, B. J. Belzer, and K. Sivakumar, "Row-column soft-decision feedback algorithm for two-dimensional intersymbol interference," *IEEE Signal Process. Lett.*, vol. 14, no. 7, pp. 433–436, Jul. 2007.

[9] Y. Chen, T. Cheng, P. Njeim, B. J. Belzer, and K. Sivakumar, "Iterative soft decision feedback zig-zag equalizer for 2D intersymbol interference channels," *IEEE J. Sel. Areas Commun.*, vol. 28, no. 2, pp. 167–180, Feb. 2010.

[10] Y. Chen and S. G. Srinivasa, "Joint self-iterating equalization and detection for two-dimensional intersymbol-interference channels," *IEEE Trans. Commun.*, vol. 61, no. 8, pp. 3219–3230, Aug. 2013.

[11] R. Wood, R. Galbraith, and J. Coker, "Two-dimensional magnetic recording (TDMR): Progress and evolution," in *Proc. 25th Magn. Rec. Conf.*, Berkeley, CA, USA, Aug. 2014.

[12] E. Hwang *et al.*, “Skew-dependent array-reader based magnetic recording (ARMR) performance evaluation with dual-reader captured waveforms,” in *Proc. 25th Magn. Rec. Conf.*, Berkeley, CA, USA, Aug. 2014.
[13] G. Mathew, E. Hwang, J. Park, G. Garfunkel, and D. Hu, “Capacity advantage of array-reader-based magnetic recording (ARMR) for next generation hard disk drives,” *IEEE Trans. Magn.*, vol. 50, no. 3, Mar. 2014, Art. ID 3300907.
[14] E. Soljanin and C. N. Georghiades, “Multihead detection for multi-track recording channels,” *IEEE Trans. Inf. Theory*, vol. 44, no. 7, pp. 2988–2997, Nov. 1998.
[15] L. M. M. Myint, P. Supnithi, and P. Tantaswadi, “An inter-track interference mitigation technique using partial ITI estimation in patterned media storage,” *IEEE Trans. Magn.*, vol. 45, no. 10, pp. 3691–3694, Oct. 2009.
[16] W. Chang and J. R. Cruz, “Inter-track interference mitigation for bit-patterned magnetic recording,” *IEEE Trans. Magn.*, vol. 46, no. 11, pp. 3899–3908, Nov. 2010.
[17] G. Han, Y. L. Guan, K. Cai, and K. S. Chan, “Asymmetric iterative multi-track detection for 2-D non-binary LDPC-coded magnetic recording,” *IEEE Trans. Magn.*, vol. 49, no. 10, pp. 5215–5221, Oct. 2013.
[18] B. Vasic and E. M. Kurtas, *Coding and Signal Processing for Magnetic Recording Systems*. New York, NY, USA: CRC Press, 2004.
[19] R. Koetter, A. C. Singer, and M. Tüchler, “Turbo equalization,” *IEEE Signal Process. Mag.*, vol. 21, no. 1, pp. 67–80, Jan. 2004.
[20] A. J. Viterbi, “Very low rate convolution codes for maximum theoretical performance of spread-spectrum multiple-access channels,” *IEEE J. Sel. Areas Commun.*, vol. 8, no. 4, pp. 641–649, May 1990.
[21] P. Patel and J. Holtzman, “Analysis of a simple successive interference cancellation scheme in a DS/CDMA system,” *IEEE J. Sel. Areas Commun.*, vol. 12, no. 5, pp. 796–807, Jun. 1994.
[22] W. Zha and S. D. Blostein, “Soft-decision successive interference cancellation CDMA receiver with amplitude averaging and robust to timing errors,” in *Proc. IEEE Global Telecommun. Conf. (GLOBECOM)*, vol. 2. Nov. 2001, pp. 743–747.
[23] R. R. Lopes and J. R. Barry, “The soft-feedback equalizer for turbo equalization of highly dispersive channels,” *IEEE Trans. Commun.*, vol. 54, no. 5, pp. 783–788, May 2006.
[24] X. Wang and H. V. Poor, “Iterative (turbo) soft interference cancellation and decoding for coded CDMA,” *IEEE Trans. Commun.*, vol. 47, no. 7, pp. 1046–1061, Jul. 1999.
[25] J. Wang and S. Li, “Soft versus hard interference cancellation in MMSE OSIC MIMO detector: A comparative study,” in *Proc. 4th Int. Symp. Wireless Commun. Syst. (ISWCS)*, Oct. 2007, pp. 642–646.
[26] J. Hagenauer, “The turbo principle: Tutorial introduction and state of the art,” in *Proc. Int. Symp. Turbo Codes Rel. Topics*, Brest, France, Sep. 1997, pp. 1–11.
[27] E. F. Haratsch, G. Mathew, J. Park, M. Jin, K. J. Worrell, and Y. X. Lee, “Intertrack interference cancellation for shingled magnetic recording,” *IEEE Trans. Magn.*, vol. 47, no. 10, pp. 3698–3703, Oct. 2011.
[28] M. Fujii, “Adaptive and iterative ITI canceller for inter-track asyncronous shingled write recording,” in *Proc. IEEE 54th Int. Midwest Symp. Circuits Syst. (MWSCAS)*, Aug. 2011, pp. 1–4.
[29] P. Kovintavewat, I. Ozgunes, E. Kurtas, J. R. Barry, and S. W. McLaughlin, “Generalized partial-response targets for perpendicular recording with jitter noise,” *IEEE Trans. Magn.*, vol. 38, no. 5, pp. 2340–2342, Sep. 2002.
[30] X.-Y. Hu. *Progressive Edge Growth (PEG) Software*. [Online]. Available: http://www.inference.phy.cam.ac.uk/mackay/PEG_ECC.html
[31] F. Gilbert, F. Kienle, and N. Wehn, “Low complexity stopping criteria for UMTS turbo-decoders,” in *Proc. 57th IEEE Semiannu. Veh. Technol. Conf. (VTC)*, vol. 4. Apr. 2003, pp. 2376–2380.

Elnaz Banan Sadeghian received the B.S. degree in electrical engineering from Shahid Beheshti University, Tehran, Iran, in 2005, and the M.S. degree in biomedical engineering from the Amirkabir University of Technology, Tehran, in 2008. She is currently pursuing the Ph.D. degree in electrical engineering with the Georgia Institute of Technology, Atlanta, GA, USA.

Her current research interests include signal processing and communication theory, including synchronization, equalization, and coding as applied to magnetic recording channels.

John R. Barry (SM’04) received the B.S. (*summa cum laude*) degree from the University at Buffalo, the State University of New York, Buffalo, NY, USA, in 1986, and the M.S. and Ph.D. degrees from the University of California at Berkeley (UC Berkeley), Berkeley, CA, USA, in 1987 and 1992, respectively, all in electrical engineering. His Ph.D. research explored the feasibility of broadband wireless communications using diffuse infrared radiation.

He has held engineering positions in the fields of communications and radar systems at Bell Communications Research, Murray Hill, NJ, USA, the IBM Thomas J. Watson Research Center, Yorktown Heights, NY, USA, Hughes Aircraft Company, Glendale, CA, USA, and General Dynamics Company, Falls Church, VA, USA, since 1985. He has co-authored a book entitled *Digital Communication—Third Edition* (Kluwer, 2004), co-edited a book entitled *Advanced Optical Wireless Communication Systems* (Cambridge University Press, 2012), and authored a book entitled *Wireless Infrared Communications* (Kluwer, 1994).

Dr. Barry was a recipient of the David J. Griep Memorial Prize in 1992, the Eliahu Jury Award from UC Berkeley, the Research Initiation Award from National Science Foundation, and the IBM Faculty Development Award in 1993. He currently serves as a Guest Editor of the special issue of the IEEE JOURNAL ON SELECTED AREAS IN COMMUNICATIONS.